Tunneling Spectroscopy of Andreev Energy Levels in a Quantum Dot Coupled to a Superconductor

R. S. Deacon,[1,*] Y. Tanaka,[2] A. Oiwa,[1,3,4] R. Sakano,[1] K. Yoshida,[3] K. Shibata,[5] K. Hirakawa,[4,5,6] and S. Tarucha[1,3,6,7]

[1]*Department of Applied Physics, The University of Tokyo, 7-3-1 Hongo, Bunkyo-ku, 113-8656, Japan*
[2]*Condensed Matter Theory Lab, RIKEN, Wako, Saitama 351-0198, Japan*
[3]*ICORP JST, 3-1 Wakamiya, Morinosato, Atsugi-shi, Kanagawa 243-0198, Japan*
[4]*JST CREST, 4-1-8 Hon-cho, Kawaguchi-shi, Saitama 332-0012, Japan*
[5]*Institute of Industrial Science, The University of Tokyo, 4-6-1 Komaba, Meguro-ku, Tokyo 153-8505, Japan*
[6]*INQIE, The University of Tokyo, 4-6-1 Komaba, Meguro-ku, Tokyo 153-8505, Japan*
[7]*QPEC, The University of Tokyo, 7-3-1 Hongo,Bunkyo-ku, 113-8656, Japan*

(Received 13 September 2009; published 19 February 2010)

The coupling of a quantum dot with a BCS-type superconducting reservoir results in an intriguing system where low energy physics is governed by the interplay of two distinct phases, singlet and doublet. In this Letter we show that the spectrum of Andreev energy levels, which capture the properties of the two phases, can be detected in transport measurements with a quantum dot strongly coupled to a superconducting lead and weakly coupled to a normal metal lead. We observe phase transitions between BCS singlet and degenerate magnetic doublet states when the quantum dot chemical potential is tuned with an electrostatic gate, in good qualitative agreement with numerical renormalization group calculations.

DOI: 10.1103/PhysRevLett.104.076805 PACS numbers: 73.63.Kv, 73.23.Hk, 74.45.+c, 74.50.+r

Electron tunneling into a BCS-type superconductor occurs through Andreev reflection in which an incident electron is converted to a Cooper pair with reflection of a hole. Andreev reflections are central to the proximity effect, in which superconducting order can ''leak'' into a contacting metal or semiconductor. When a quantum dot (QD) is coupled to a superconductor the Andreev reflection requires that electron pairs occupy the QD and the proximity effect is therefore sensitive to correlation effects such as Coulomb interaction [1] and the many-body Kondo effect [2–5]. While there have been a wide range of experimental studies on the superconductor-QD-superconductor (S-QD-S) system [6–15], the hybrid normal-QD-S (N-QD-S) system is relatively experimentally unexplored [16]. In the weak coupling limit it has been shown that a QD Josephson junction with strong electron-electron interaction exhibits positive and negative Josephson supercurrent [7,9,10], that is a 0 or π junction, for even and odd electron occupation. The nondissipative supercurrent in QD Josephson junctions [17] is mainly carried by Andreev localized states, often called Andreev bound states. Underlying the dramatic change in transport properties at the 0-π junction transition is a phase transition between two distinct ground states (GSs) [2,18–21]. The 0 junction has a BCS-like nonmagnetic singlet GS. In the case of a π junction the GS is a degenerate (so-called magnetic) doublet state which describes free magnetic moments. Recently Andreev bound states were proposed as a novel Andreev level qubit system [22], fueling interest in direct study [23]. S-QD-S devices are unsuitable for such study as low bias dissipative transport is governed by high order multiple Andreev reflections [24] between the two superconductor-QD interfaces resulting in a complex spectrum of resonances from which the local energy spectrum is difficult to extract and only indirectly observed in the nondissipative supercurrent. The N-QD-S devices considered in this Letter allow a more direct study of Andreev energy levels through Andreev tunneling spectroscopy [25] using a weakly coupled N lead.

The transport characteristics of a conventional N-S junction are well described by the BTK model [26] in which the junction is characterized by a single tunneling rate through the barrier. For a typical N-S junction the tunnel rate is low, Andreev conductance is suppressed, and the transport reflects the density of states of the S lead. For a N-QD-S system [Fig. 1(c)] both the normal lead $\Gamma_N/\hbar$ and superconducting lead $\Gamma_S/\hbar$ tunnel rates must be considered for a complete description of the transport. The energy dependent transmission of the QD junction can result in pronounced subgap structure [27], which is sensitive to the QD energy level ε_d and reflects the superconducting order induced upon the QD through the proximity effect [5,19]. At low temperatures, below a characteristic Kondo temperature (T_K), interplay between Kondo correlations and BCS superconductivity becomes important [6,15,18,21]. In this Letter we focus on devices with large tunnel coupling asymmetry favoring the S lead in which the Kondo effect is suppressed by strong proximity effect.

Devices are fabricated using uncapped self-assembled InAs QDs, with typical diameters of $\sim$100 nm, contacted with a nanogap electrode technique [28]. A degenerately Si-doped GaAs layer 300 nm below the surface is used as a backgate. Additional fabrication details may be found in Ref. [15]. Nanogap electrodes were fabricated using a two step e-beam lithography and e-beam evaporation procedure to deposit one Ti/Al (5 nm/150 nm) S lead and one

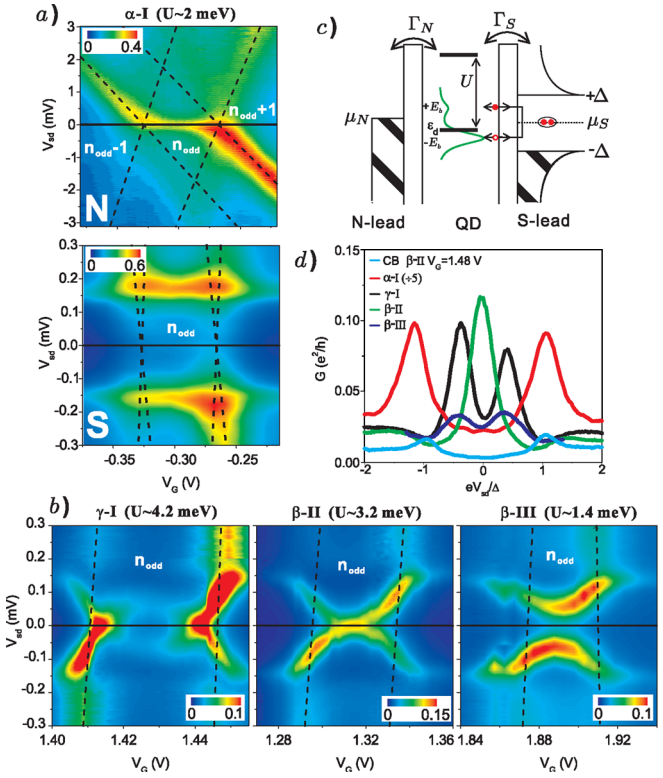

FIG. 1 (color online). (a) False color plot of N state ($B = 220$ mT) and S state ($B = 0$ mT) differential conductance ($G = dI/dV_{sd}$) for region α-I ($\Gamma_N/\Gamma_S \sim 12$) with odd electron number n_{odd}. The color scale is in units of e^2/h. Dashed lines mark the Coulomb diamond from which the charging energy $U \sim 2$ meV is estimated. (b) False color plots of $G(V_{sd}, V_G)$ for three n_{odd} regions all with high asymmetry $\Gamma_S/\Gamma_N > 40$. V_{sd} scales are identical to that in (a) in the S state. Charging energies are $U \sim 4.2$ meV, $U \sim 3.4$ meV, and $U \sim 1.4$ meV for γ-I, β-II, and β-III, respectively. The intercept of dashed lines with $V_{sd} = 0$ indicates the zero-bias resonance conditions. (c) Schematic of the N-QD-S system. Andreev reflections mix electron-hole states on the QD and generate two broadened Andreev energy levels in the local energy spectrum pictured at $+E_b$ and $-E_b$. (d) Plots of $G(eV_{sd}/\Delta)$ for the center of n_{odd} regions alongside an example of the transport in the even occupation Coulomb blockade (CB) regime.

Ti/Au (10 nm/50 nm) N lead. All measurements were performed in a He^3-He^4 dilution refrigerator with base temperature of $T \sim 30$ mK using conventional lock-in measurement techniques ($V_{\mathrm{ac}} \sim 3$ μV). We measure two devices labeled α and β. After measurement of device β the dilution refrigerator temperature was cycled, after which the device characteristics were changed. Data for device β following the thermal cycle we label as device γ for easy reference. We label the odd occupation regions in each device with roman numerals. Note however that the numerals are arbitrary and do not reflect the electron number which we estimate to be a few tens. Tuning the electron occupation of the QD using the backgate also alters the parameters, $\Gamma_{S,N}$, energy level spacing $\Delta\varepsilon$, and charging energy U, allowing study of different regimes of behavior in a single device [28]. Devices are characterized in the N state by applying an in plane magnetic field greater than the Al lead critical field ($B_c \sim 200$ mT) [Fig. 1(a)]. The even or odd electron occupation is confirmed through the evolution of Coulomb peaks in a high magnetic field ($B \gg B_c$). Device parameters vary in the range $\Delta\varepsilon \sim 2$–8 meV and $U \sim 1$–5 meV.

Low bias differential conductance ($G = dI/dV_{sd}$) in the S state for region α-I [Fig. 1(a)] is strongly suppressed. In even occupation regions we observe resonant peaks at $|eV_{sd}| \sim 152$ μeV which we attribute to single quasiparticle tunneling where the chemical potential of the N lead and the edge of the superconducting energy gap are aligned; i.e., $|eV_{sd}| = \Delta$. From these features we estimate the superconducting transition temperature, $\Delta = 1.76 k_B T_c \sim 152$ μeV, as $T_c \sim 1$ K. In this regime the transport is well described by a low transparency tunnel junction in the conventional BTK theory [26]. We estimate the conditions for resonance between the discrete QD levels and the lead chemical potentials, $\mu_{N,S} \sim \varepsilon_d$ and $\mu_{N,S} \sim \varepsilon_d + U$, by fitting transport resonance peaks for $|eV_{sd}| > \Delta$ [29] [see dashed lines in Figs. 1(a) and 1(b)]. The relative tunnel coupling asymmetry of devices is determined through consideration of the N state stability diagram [29]. For region α-I, Fig. 1(a), we determine that $\Gamma_N > \Gamma_S$ in contrast to regions in device β and γ where $\Gamma_S > \Gamma_N$. In Fig. 1(d) we plot $G(V_{sd})$ at the center of each n_{odd} region for comparison. We observe that for $\Gamma_S > \Gamma_N$ single quasiparticle tunneling features are suppressed relative to the subgap features in good agreement with predictions for the noninteracting N-QD-S system [27,29]. We attribute the subgap transport peaks observed when $\Gamma_S > \Gamma_N$ to resonant Andreev transport through Andreev energy levels, formed through electron-hole mixing of the QD energy level. For regions with high U such as γ-I ($U \sim 4.2$ meV) we observe a crossing of the subgap transport resonances at $V_{sd} = 0$ in the n_{odd} region near the zero-bias resonance points. For region β-II where $U \sim 3.4$ meV the subgap resonance crossing point occurs at the center of the n_{odd} region. Finally, for region β-III with small $U \sim 1.4$ meV the subgap resonances never cross.

For comparison with experimental results the local energy spectrum has been calculated for the Anderson impurity coupled to a superconducting reservoir using the numerical renormalization group (NRG) method detailed in Ref. [19]. The system has two possible ground states, a doublet and a BCS-like singlet (which is a superposition of doubly occupied and empty states). Calculations of the single particle spectral function at the QD reveal a pair of sharp peaks or Andreev energy levels which indicate the excitation between the GS and excited state through addition of an electron ($E_b > 0$) or hole ($E_b < 0$) at an energy E_b relative to the Fermi energy. Note that both Andreev energy levels correspond to the same excited state. When

$E_b = 0$ the excited state (Andreev bound state) and GS are degenerate. Figure 2(a) shows plots of Andreev level energies as a function of ε_d for comparison with experiment. When U is small the system GS is always a BCS-like singlet and the excited state is a magnetic doublet. For sufficiently large U, however, a phase transition between BCS-like singlet GS and magnetic doublet GS may be achieved by tuning ε_d. This transition occurs at the crossing of Andreev energy levels (where GS and excited state are degenerate) and is observed as an abrupt change in the spectral weights of the two features as shown in Fig. 2(b). When the phase transition occurs, the GS of the new phase is the excited state of the previous phase. For a system with high U (circles) the transition to magnetic doublet GS occurs near the resonance conditions while for intermediate U (squares) the transition is shifted toward the center of the n_{odd} region until finally for low U (stars) the GS is always BCS singlet and the Andreev energy levels are always separated. The QD-S system considered is analogous to a S-QD-S junction in equilibrium with the superconducting phase difference between reservoirs set to zero. Similar theoretical treatments which calculate the transport supercurrent for the S-QD-S system [20,21] find that in the magnetic doublet GS regime the critical current is strongly suppressed, which may be attributed to the reduced spectral weights of the Andreev energy levels. Recent experiments have identified the 0-π junction transition by observing abrupt suppression of the supercurrent at the phase transition point [7,11].

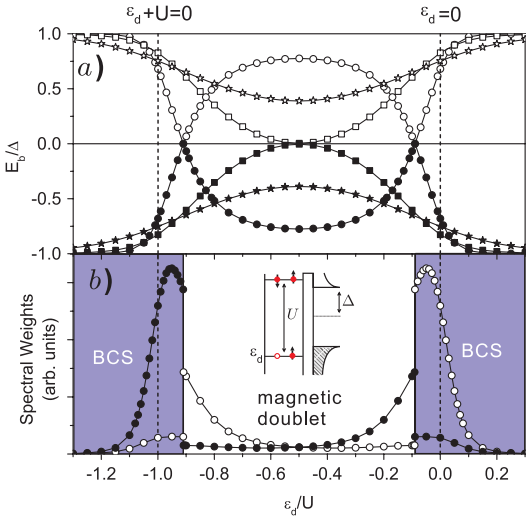

FIG. 2 (color online). (a) NRG calculation of the Andreev energy level spectrum as a function of ε_d for the QD-S system following the method in Ref. [19]. Simulation parameters are selected for comparison with experimental data in Fig. 1(b) (circles) $U/\Delta = 28$, $\Gamma_S/\Delta = 1.5$, (squares) $U/\Delta = 23$, $\Gamma_S/\Delta = 3.4$, (stars) $U/\Delta = 9.3$, $\Gamma_S/\Delta = 2.8$. All simulations are at $T = 0$ K. (b) Plot of spectral weight of the two Andreev energy levels (○ for $E_b > 0$ and ● for $E_b < 0$) for $U/\Delta = 28$, $\Gamma_S/\Delta = 1.5$. The BCS singlet and magnetic doublet GS regimes are indicated by the shaded regions. Vertical dashed lines indicate the resonance conditions for which the QD energy levels are aligned with the Fermi energy, $\varepsilon_d = 0$ and $\varepsilon_d + U = 0$. Inset: Schematic of the QD-S system considered.

In the case of the N-QD-S system the Andreev energy levels are not spectroscopically sharp but broad resonances as the system is no longer fully gapped due to interactions with the N lead [4]. The Andreev energy levels are then only well resolved in the local spectral function if $\Gamma_S \gg \Gamma_N$ and $\Gamma_N \ll \Delta$. Furthermore, interplay between Kondo correlations with the N lead and proximity effect with the S lead determine the QD GS. For finite Γ_N the Kondo state will always appear at zero temperature. The phase transition from BCS singlet to magnetic doublet state is only realized if the system temperature $T > T_K$. If $T \lesssim T_K$ a crossover from Kondo-like singlet to BCS superconducting singlet GS is expected [4]. The NRG theory presented only reveals the equilibrium energy spectrum for the QD-S system; however, when $\Gamma_S \gg \Gamma_N$ and $\Gamma_N \ll \Delta$ similar , albeit broadened, Andreev energy levels will be observed in the N-QD-S energy spectrum with qualitatively the same behavior. The nature of the Andreev transport channel does not allow for spectroscopic measurements of the electron and hole Andreev energy levels individually as the superposition of local spectral function for electrons and holes determines the Andreev conductance [29]. We expect therefore that in the noninteracting system the conductance from Andreev processes as a function of V_{sd} is symmetric with respect to $V_{sd} = 0$ even when the local spectral function is asymmetric in energy. In regions displaying subgap features we evaluate $\Gamma_S/\Gamma_N > 40$ with a total tunnel coupling of $\Gamma \sim 0.2$–1 meV such that $\Gamma_N < 25$ μeV. In these regions, in which the Kondo screening is suppressed in the S state, the NRG calculations [4,19] show excellent qualitative agreement with the experimentally observed subgap transport resonances [Fig. 1(b)].

The predicted abrupt change in spectral weights of the Andreev energy levels can also be observed in experiment, in particular, in region α-II for which the subgap resonances were well resolved (indicating a small Γ_N). In Fig. 3(a) we examine in detail the transition between singlet and doublet GSs in region α-II where we observe that following the crossing of the subgap features in the n_{odd} region the peak conductance of subgap resonances is suppressed. This is further highlighted by plotting the peak conductance of the subgap features in Fig. 3(b). For comparison simulations of the energy spectrum for a similar QD-S system are presented in Figs. 3(c) and 3(d). In transport with a weakly coupled N lead the relative conductance of Andreev transport resonances may be very crudely estimated using the product of the electron and hole spectral weights [stars in Fig. 3(d)]. We find good qualitative agreement between the theoretical expectation and experimental results. In experiment the asymmetry in positive and negative bias subgap peak conductance for $V_G < 0.79$ V is unexpected, but may originate from out of

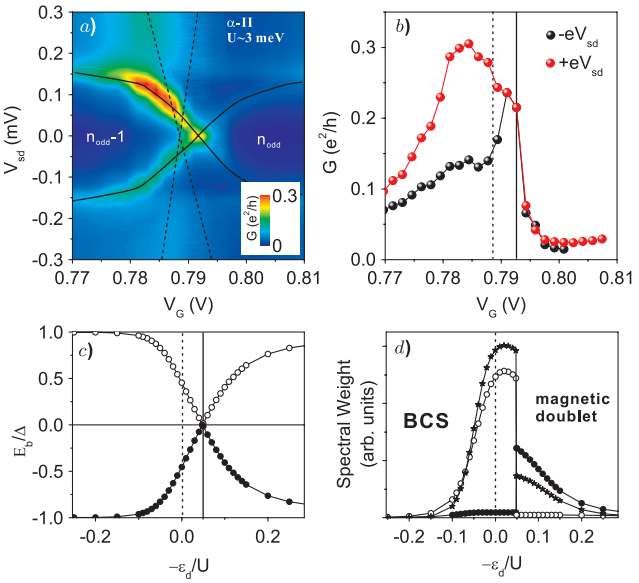

FIG. 3 (color online). (a) False color plot of differential conductance centered on the crossing of Andreev resonances states for α-II, $\Gamma_S/\Gamma_N \sim 50$, and $U \sim 3$ meV. The resonance conditions of the discrete QD level with the lead chemical potentials are marked with dashed lines. Solid lines indicate the subgap transport resonances. (b) Plots of the peak conductance of subgap transport resonances [following solid lines in (a)]. The solid vertical line indicates the phase transition. (c) Andreev energy level spectrum calculated for the QD-S system with $U/\Delta = 20$ and $\Gamma_S/\Delta = 0.7$ using the NRG method. (d) Spectral weights of the electron (○) and hole (●) Andreev energy levels alongside the product of the two spectral weights (×65) (★). Note that simulations are of the energy spectrum of the QD-S system in equilibrium and are not of transport.

equilibrium electron-electron interactions, specifics of the normal lead density of states or single quasiparticle tunneling which persists within the superconducting gap due to smearing of the superconducting gap edge caused by impurities and the presence of the 5 nm Ti adhesion layer.

In summary, we perform tunneling spectroscopy of Andreev energy levels in single self-assembled InAs quantum dots contacted with normal and superconducting leads. The crossing of subgap transport resonances indicates a phase transition between BCS singlet and magnetic doublet states in excellent qualitative agreement with numerical calculations [4,19]. The Andreev energy level is a key concept in the theoretical treatment of nanoscale Josephson junctions. The present study shows that Andreev energy levels can be probed in simple transport measurements and that they are a sensitive indicator of the local quantum dot correlations.

We acknowledge valuable discussions with N. Nagaosa, A. Oguri, A. Levy-Yeyati, and Y. Yamada. We acknowledge financial support from the Japan Society for the Promotion of Science, Grant No. P07328 (R. S. D), the Special Postdoctoral Researchers Program of RIKEN (Y. T.), and Grant-in-Aid for Scientific Research S (No. 19104007) and A (No. 21244046).

*russell@meso.t.u-tokyo.ac.jp

[1] K. Kang, Phys. Rev. B **58**, 9641 (1998).
[2] E. Vecino, A. Martin-Rodero, and A. L. Yeyati, Phys. Rev. B **68**, 035105 (2003).
[3] J. Cuevas, A. L. Yeyati, and A. Martin-Rodero, Phys. Rev. B **63**, 094515 (2001).
[4] Yoichi Tanaka, N. Kawakami, and A. Oguri, J. Phys. Soc. Jpn. **76**, 074701 (2007).
[5] T. Domanski and A. Donabidowicz, Phys. Rev. B **78**, 073105 (2008).
[6] M. Buitelaar, T. Nussbaumer, and C. Schönenberger, Phys. Rev. Lett. **89**, 256801 (2002).
[7] H. Jorgensen *et al.*, Nano Lett. **7**, 2441 (2007).
[8] K. Grove-Rasmussen, H. I. Jorgensen, and P. Lindelof, New J. Phys. **9**, 124 (2007).
[9] J. van Dam *et al.*, Nature (London) **442**, 667 (2006).
[10] J. Cleuziou *et al.*, Nature Nanotech. **1**, 53 (2006).
[11] A. Eichler *et al.*, Phys. Rev. B **79**, 161407(R) (2009).
[12] A. Eichler *et al.*, Phys. Rev. Lett. **99**, 126602 (2007).
[13] P. Jarillo-Herrero, J. van Dam, and L. Kouwenhoven, Nature (London) **439**, 953 (2006).
[14] T. Sand-Jespersen *et al.*, Phys. Rev. Lett. **99**, 126603 (2007).
[15] C. Buizert *et al.*, Phys. Rev. Lett. **99**, 136806 (2007).
[16] M. Gräber *et al.*, Nanotechnology **15**, S479 (2004).
[17] C. Beenakker and W. van Houten, *Single-Electron Tunneling and Mesoscopic Devices* (Springer, Berlin, 1992).
[18] O. Sakai *et al.*, J. Phys. Soc. Jpn. **62**, 3181 (1993).
[19] J. Bauer, A. Oguri, and A. C. Hewson, J. Phys. Condens. Matter **19**, 486211 (2007).
[20] A. Oguri, Yochihide Tanaka, and A. Hewson, J. Phys. Soc. Jpn. **73**, 2494 (2004).
[21] C. Karrasch, A. Oguri, and V. Meden, Phys. Rev. B **77**, 024517 (2008).
[22] A. Zazunov *et al.*, Phys. Rev. Lett. **90**, 087003 (2003).
[23] J. Skoldberg *et al.*, Phys. Rev. Lett. **101**, 087002 (2008).
[24] M. Buitelaar *et al.*, Phys. Rev. Lett. **91**, 057005 (2003).
[25] M. Governale, M. Pala, and J. König, Phys. Rev. B **77**, 134513 (2008).
[26] G. Blonder, M. Tinkham, and T. Klapwijk, Phys. Rev. B **25**, 4515 (1982).
[27] V. Khlus, A. Dyomin, and A. Zazunov, Physica (Amsterdam) **214C**, 413 (1993).
[28] M. Jung *et al.*, Appl. Phys. Lett. **87**, 203109 (2005).
[29] See supplementary material at http://link.aps.org/supplemental/10.1103/PhysRevLett.104.076805 for simulations of the noninteracting system.